TERA

NORTHEAST UTILITIES

P.O. BOX 270
HARTFORD, CONNECTICUT 06101
(203) 666-6911

October 22, 1979

Docket No. 50-336

Director of Nuclear Reactor Regulation
Attn: Mr. R. Reid, Chief
Operating Reactors Branch #4
U. S. Nuclear Regulatory Commission
Washington, D. C. 20555

References: (1) W. G. Counsil letter to R. Reid dated September 28, 1979.
(2) Telecopy from E. L. Conner for Additional Information dated October 16, 1979.
(3) W. G. Counsil letter to R. Reid dated August 22, 1979.

Gentlemen:

Millstone Nuclear Power Station, Unit No. 2
Feedwater System Piping

In response to Reference (2), a meeting was held in Bethesda on October 19, 1979 to discuss the NRC request for additional information regarding Reference (1). As a result of the October 19, 1979 meeting, additional information enclosed herein is submitted in response to the NRC Staff request regarding the ASME Section XI applicability of the existing feedwater piping system linear indications.

Attachment 1 provides a discussion of the methods of analyses including the fatigue crack growth analysis and the determination of the critical flaw size. Attachment 2 provides the assessment of crack growth for the worst feedwater line flaw considering both the design basis transients and the thermal loading conditions observed from the Millstone Unit No. 2 instrumentation data. Attachment 3 provides the critical flaw sizes for part-through wall cracks and through-wall cracks using the established loading conditions.

In reference to the submitted information, we note the following:

(1) The stresses calculated and presented in Tables 2 through 5 of Attachment 2 are conservative, because they were generated from a model meant to umbrella a number of different feedwater line observations. Specifically, the maximum stresses in Table 4 (Attachment 2) should be multiplied by 0.753 for specific applicability to Millstone Unit No. 2.

1208 251

7910250 279

Thus, the largest value of the stress intensity factor (K) which would result from a 0.100 inch deep flaw is 34.0 ksi $\sqrt{in.}$

(2) The results of the detailed piping integrity analyses confirm that the ductile failure limits of ASME Section XI are met. However, the specific LEFM criteria for flaw evaluation in ASME Section XI — IWB-3600 is not applicable to the feedwater piping system.

(3) Using the results of the fatigue crack growth analysis and comparing them to the established critical flaw size, it is concluded that there is a large safety margin.

It is, therefore, concluded that the existing condition of the Millstone Unit No. 2 feedwater piping system is in compliance with the applicable criteria of the ASME Boiler and Pressure Vessel Code as documented in Reference (3). Additional information presented at the October 19, 1979 meeting will be submitted by October 24, 1979.

We request your immediate attention to this matter and trust this information satisfactorily dispositions the Staff's concerns.

Very truly yours,

NORTHEAST NUCLEAR ENERGY COMPANY

W. G. Counsil
Vice President

Attachments

DOCKET NO. 50-336

ATTACHMENT 1

MILLSTONE NUCLEAR POWER STATION, UNIT NO. 2

FEEDWATER SYSTEM PIPING

OCTOBER, 1979

METHODS OF ANALYSIS

In this work, the observed indication is treated as a sharp crack, and analyzed as to its behavior in future service. Growth due to further cycling is evaluated in fatigue crack growth analyses, and then the final flaw size is compared with the critical flaw size for normal and upset and other operating conditions. In this section, the methods used in these analyses will be detailed.

(1) FATIGUE CRACK GROWTH ANALYSIS

The fatigue crack growth analysis was conducted in the same manner as suggested by ASME Section XI, Appendix A. The operating transients which affect the feedwater line are all considered, and scheduled out over a 40-year period. The initial flaw depth assumed was that of the original indication, but slightly greater depths were also considered, to give further information.

Crack tip stress intensity factors (K_I) were calculated using an expression for a continuous flaw oriented circumferentially at the inside surface of the pipe. The stresses were linearized through the pipe wall thickness, and used to calculate K_I and ΔK_I. The fatigue crack growth for any single transient was calculated from a crack growth rate law determined to be applicable for the materials of the pipe, exposed to a water environment.

(2) DETERMINATION OF CRITICAL FLAW SIZE

The feedwater piping and welds are fabricated from carbon steel and operate at elevated temperature. A great deal of study of the failure aspects of piping and tubing have been undertaken in recent years and considerable experimental data are now available. A large number of failure theories have been developed, both analytically based and empirically based, with varying degrees of success. This section will briefly review various types of theories, and provide the basis for use of the plastic insta method in predicting the critical flaw size for the area of interest.

Fracture mechanics was first developed for the case of low energy fracture which involved small deformations. This is termed brittle fracture, and the theory is called linear elastic fracture mechanics (LEFM). The theory is generally applicable only to brittle materials for example high strength alloys and those which operate at low temperature. A further requirement for strict applicability of LEFM is the presence of a heavy section, where the stress state is plane strain. Failure in these materials and geometries is abrupt, and the crack propagates at speeds approaching the speed of sound. The theory predicts that failure will occur when the applied stress intensity factor exceeds the material's fracture toughness, or resistance to failure.

There is a large range of materials and geometries where the conditions necessary for linear elastic or brittle fracture do not exist. This happens in lower strength carbon steels, stainless steels, and Inconel, particularly those with high ductility, and also in structures with thin sections with low constraint on the opening of a crack. A good example of this geometry is piping and tubing. In this case, once a crack is loaded to the point where it begins to propagate, failure does not occur at once. Instead, as the crack propagates, the plastic zone ahead of the crack grows with the crack, and a steady increase in the magnitude of the load becomes necessary to overcome the increasing resistance of the material to fracture. Consequently, a toughness oriented single parameter fracture criterion becomes totally inadequate to deal with the problem of ductile failure.

A number of concepts have been developed for the prediction of ductile failure, and these are reviewed in detail in a number of recent works, for example references 1, 2, 3, and 4. Two of the more popular parameters for ductile fracture are the J-integral[5] and the crack opening displacement (COD)[6] concept. These parameters have been shown to be successful at predicting the onset of ductile crack propagation, but are only now being extended to the prediction of final failure. Extensions to the point of unstable propagation and final failure have thus far been centered on R-curve technology[7] and development of the Tearing Modulus concept by Paris[8] is an extension of this trend.

Based on the level of Charpy energy at 0°F from tests of the actual material as well as experience with results from similar materials, the transition from brittle to ductile behavior should occur at room temperature or below.

The operating regime for the feedwater lines as well as their material and geometry places the fracture mode squarely in the large strain - general yield regime. As such, the crack will generally not become unstable until beyond the point where the entire remaining ligament becomes plastic. If this occurs, the failure will be well predicted by the plastic limit load of the structure, corrected to account for the material strain hardening behavior.

There is considerable body of experimental data which shows that the governing mode of failure for ductile cracked pipes and tubes is that of plastic instability. Several series of experiments on piping geometries were completed by both General Electric and Battelle Memorial Institute as early as 1968, and these results, as well as other more recent results are well-predicted by the plastic instability method, as discussed in Appendix A. Therefore, the approach taken in this analysis was to evaluate the propensity for failure by the plastic instability mode.

(3) SAFETY ASSESSMENT

Once the growth of the assumed crack-like defect has been calculated, the resulting flaw is compared with the critical flaw size to determine the margins of safety for further operation. This assessment method is similar to that used in Section XI of the ASME code, but the details of the calculations are different, especially the critical flaw size calculation for ductile failure. Note that there are presently no rules or guidelines in the ASME code for such calculations in secondary systems. The assessment method used is, therefore, based on good engineering practice.

APPENDIX A

DETERMINATION OF THE MOMENT CAPACITY OF PRESSURIZED PIPING WITH CIRCUMFERENTIALLY ORIENTED THROUGH WALL FLAWS

A straight section of pipe with a circumferentially oriented through wall flaw; as shown in Figure A-1, is considered. It is assumed that plane sections remain plane during deformation, and that the flaw is not too large in comparison with the pipe circumference. For flaw lengths which approach one-half of the circumference, the present method is not accurate.

The pipe is loaded by internal pressure, P, an axial force, F, and a bending moment, M. Because of the bending moment, the axial stress will be compressive somewhere in the cross section. The point of demarcation between tensile and compressive stresses is the neutral axis, as shown in Figure A-1. To determine the location of the neutral axis, the axial force on the pipe from the internal pressure and other loads, N, is equated to the integrated stresses over the cross-sectional area of the pipe, N_o as follows:

$$N = P\pi R^2 + F \qquad \text{(A-1)}$$

Where:

P = Internal Pressure

R = Mean Radius of the Pipe

F = Other axial force (if any)

$$N_o = 2\int_{-\beta}^{\frac{\pi}{2}-\alpha} \sigma f \, Rt \, d\theta + 2\int_{-\frac{\pi}{2}}^{-\beta} \left(\frac{PR}{t} - \sigma f \, Rt \, d\theta\right) \qquad \text{(A-2)}$$

Where:

t = Pipe Thickness

σf = Flow Stress = $0.4\ (\sigma_{ys} + \sigma_u)$

α = Crack angle as shown in Figure A-1.

β = Angle to located neutral axis, Figure A-1.

Equating the quantities in (A-1) and (A-2) leads to the definition of the neutral axis which is:

$$\beta = \frac{\sigma_f \, t \, \alpha - \frac{F}{2}}{2 \, \sigma_f \, t - PR} \qquad \text{(A-3)}$$

Figure A-1 also illustrates that the angles α and β are related at the limit moment; therefore, equating areas above and below the neutral axis results in the following:

$$\alpha = 2\beta \qquad \text{(A-4)}$$

The fully-plastic limit moment capacity, M_b, is obtained by taking moments about the neutral axis as follows:

$$M_b = 2 \int_{-\beta}^{(90 - \alpha)} R_m^2 t \, \sigma_f \sin\theta \, d\theta - \int_{(\pi + \beta)}^{(2\pi - \beta)} R_m^2 \, t \, \sigma_f \sin\theta \, d\theta \qquad \text{(A-5)}$$

Where: $\sigma_f = 0.4 \, (\sigma_{ys} + \sigma_u)$, that is, σ_f is the flow stress.

After integration and substitution of the limits, the moment capacity for a pipe without internal pressure is found to be:

$$M_b = 2\sigma_f \, R_o^3 \, t \, (2 \cos\beta - \sin\alpha) \qquad \text{(A-6)}$$

For simple pressure loading with no bending, the limiting force is equal to:

$$N_o = 2 \, (\pi - \alpha) \, R_m \, t \, \sigma_f \qquad \text{(A-7)}$$

For any arbitrary pressure, P, the force produced is:

$$N = \pi R_i^2 \, P \qquad \text{(A-8)}$$

Then, the ratios of axial force to limit axial force and moment to limit moment are defined as follows:

$$n = \frac{N}{N_o} \qquad m = \frac{M}{M_b} \tag{A-9}$$

Since the internal pressure and bending moment interact, the combined effect will cause a reduction in the moment capacity M_b to M. From Hodge's interaction theory(1). The corrected limit moment is determined from:

$$M = (1 - n^2)\, M_b \tag{A-10}$$

Substituting for all the parameters from equations (A-6) through (A-9), we obtain:

$$M_L = \frac{4\,(\pi - \alpha)^2\, R_m^{\,2}\, t^2\, \sigma_f^{\,2} - \pi^2\, R_i^{\,4}\, P^2}{2\,(\pi - \alpha)^2\, R_m^{\,2}\, t\, \sigma_f}\; [R_o^{\,2}\,(2\cos\beta - \sin\alpha)] \tag{A-11}$$

---

(1) Hodge, P. G., Plastic Analysis of Structures. McGraw-Hill Book Company, 1959, pp. 130 - 190.

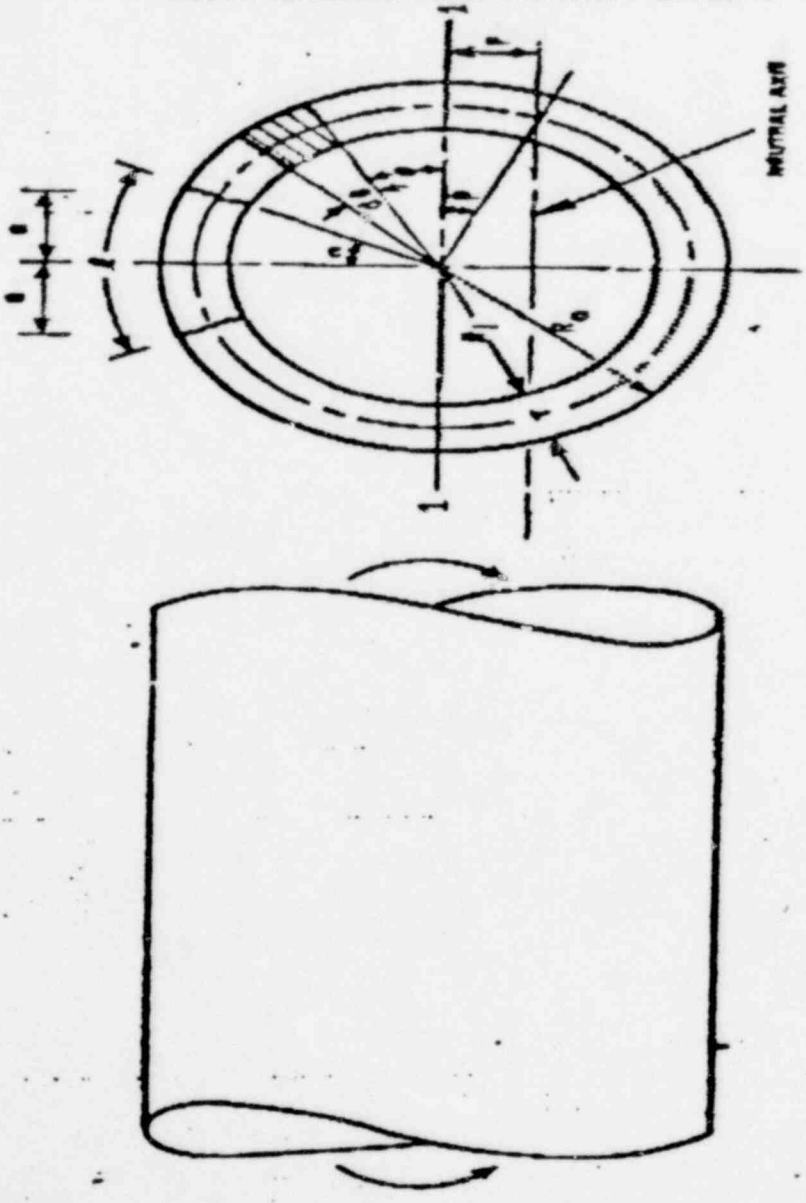

Figure A-1. Pipe With a Through-Wall Crack in Bending

DOCKET NO. 50-336

ATTACHMENT 2

MILLSTONE NUCLEAR POWER STATION, UNIT NO. 2

FEEDWATER SYSTEM PIPING

OCTOBER, 1979

ASSESSMENT OF GROWTH OF FEEDWATER LINE FLAWS

MILLSTONE II

W.H. Bamford

The purpose of this work is to estimate the future growth of a flaw located in the counterbore region near the feedwater nozzle safe-end-to-pipe weld. The flaw of interest has been confirmed by UT to be approximately 0.10 inches deep, and oriented circumferentially.

As a result of the location of this flaw, instrumentation was installed to monitor the temperature fluctuations in one loop. Results showed that in a certain flow rate range the water stratifies, producing significant stresses which are potentiall important for crack growth. The types of stratification produced were typical of those observed in other plants, but not as severe. The observed stratifications were classified under five different types, as shown in Figure 1. The temperature difference from top to bottom of the pipe for profile 1 was measured at about 350°F, whereas for other plants it has been found to be as high as 450°F.

A three dimensional finite element stress analysis has been completed for each of the five temperature profiles in Figure 1, and transient studies have shown that the five profiles represent limiting conditions compared with the stress results obtained for any transient step in between the profiles.

To accomplish a fatigue crack growth analysis, the system design transients for normal, upset and test conditions were combined with the cycles of stress from stratification, which occurs during hot standby operation. As shown in Figure 2, there are approximately nine cycles of various degrees which for the purpose of this analysis, we will assume, occur each time hot standby occurs.

A tabulation of the cycle types used in the crack growth analysis, along with applicable stresses, is provided in Table 1. Tables 2 through 5 show the stresses at various locations around the pipe as a result of the stratification.

The actual stresses from the three dimensional analysis were used for the fatigue crack growth analysis, except in two cases, where compressive stresses far exceeded the yield stress in compression. The location is at the top of the pipe, and the condition occurs only when the pipe is nearly filled with cold water (profile 1) at low flow. For this case, tensile residual stress values were assumed to exist, equal to the yield strength. This is seen at locations 1 and 2 in Tables 2 and 4. This assumption is considered to be extremely conservative.

Crack growth was calculated at each of thirteen locations around the pipe for periods of 1, 2, 3 and 4 years, assuming an initial flaw of 0.100 inches deep, extending entirely around the inside of the pipe.

A fatigue crack growth law which accounts for mean stress or R ratio (σmin./ σ max.) as well as the presence of the water environment was used. The law is shown in Figure 3.

Results of the crack growth analysis are shown in Table 6, for each of the locations considered. These results show that the observe flaws will not grow significantly during the next years service. The final flaw size for the worst location is a factor of 5 smaller than the critical flaw size for the pipe, as shown in Figure 4.

FIGURE 1. STEADY STATE TEMPERATURE DISTRIBUTIONS

[illegible] -

[illegible] -

D.C. COOK, LOOP 3
7/2/79 0 HRS
(1)

D.C. COOK, LOOP 3
EVENT 20, 0 MIN.
(2)

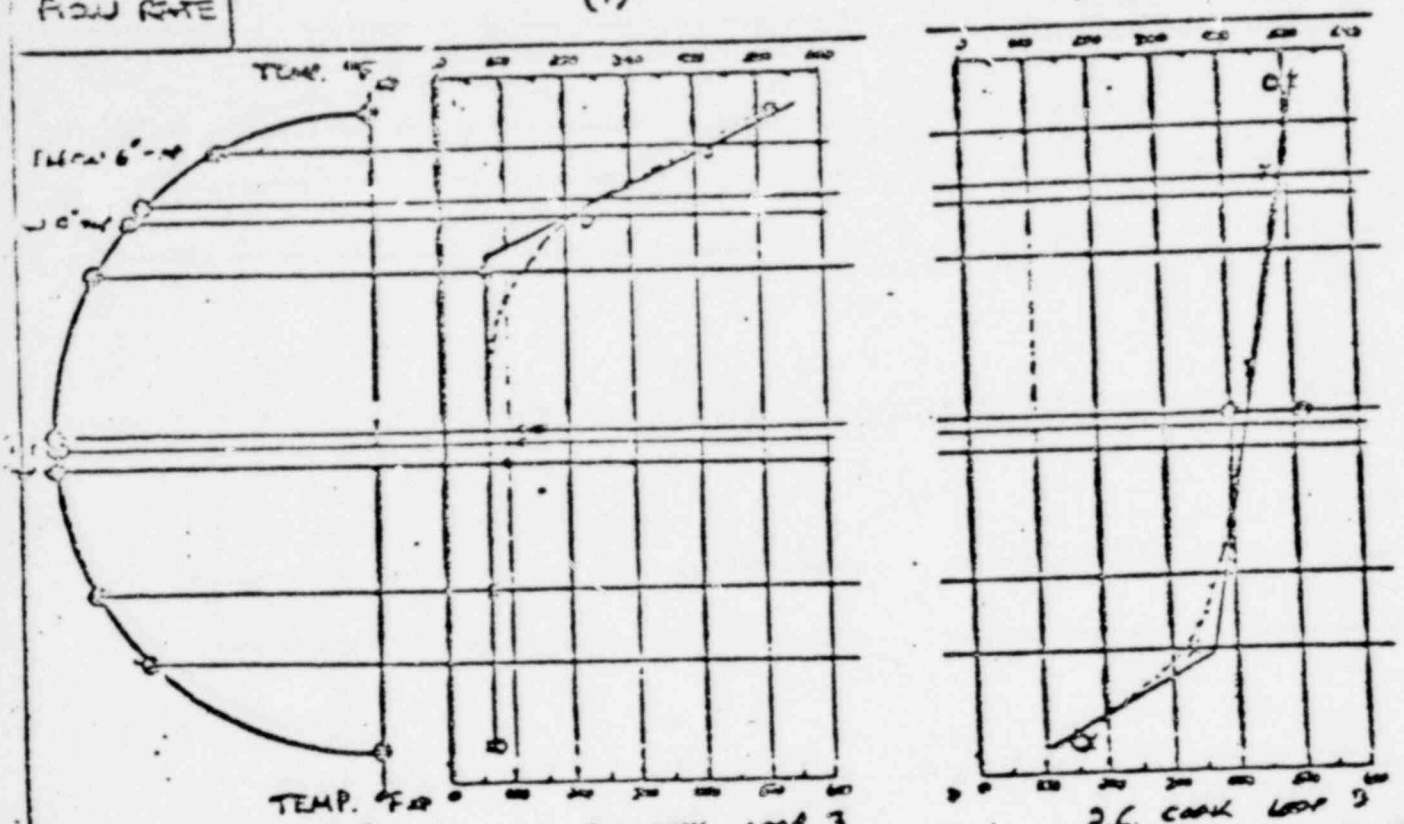

D.C. COOK, LOOP 3
7/3/79 09:30 HRS
(3)

D.C. COOK, LOOP 3
EVENT 31, 20 MINS
(4)

D.C. COOK LOOP 3
7/1/79 07.30 HRS
(5)

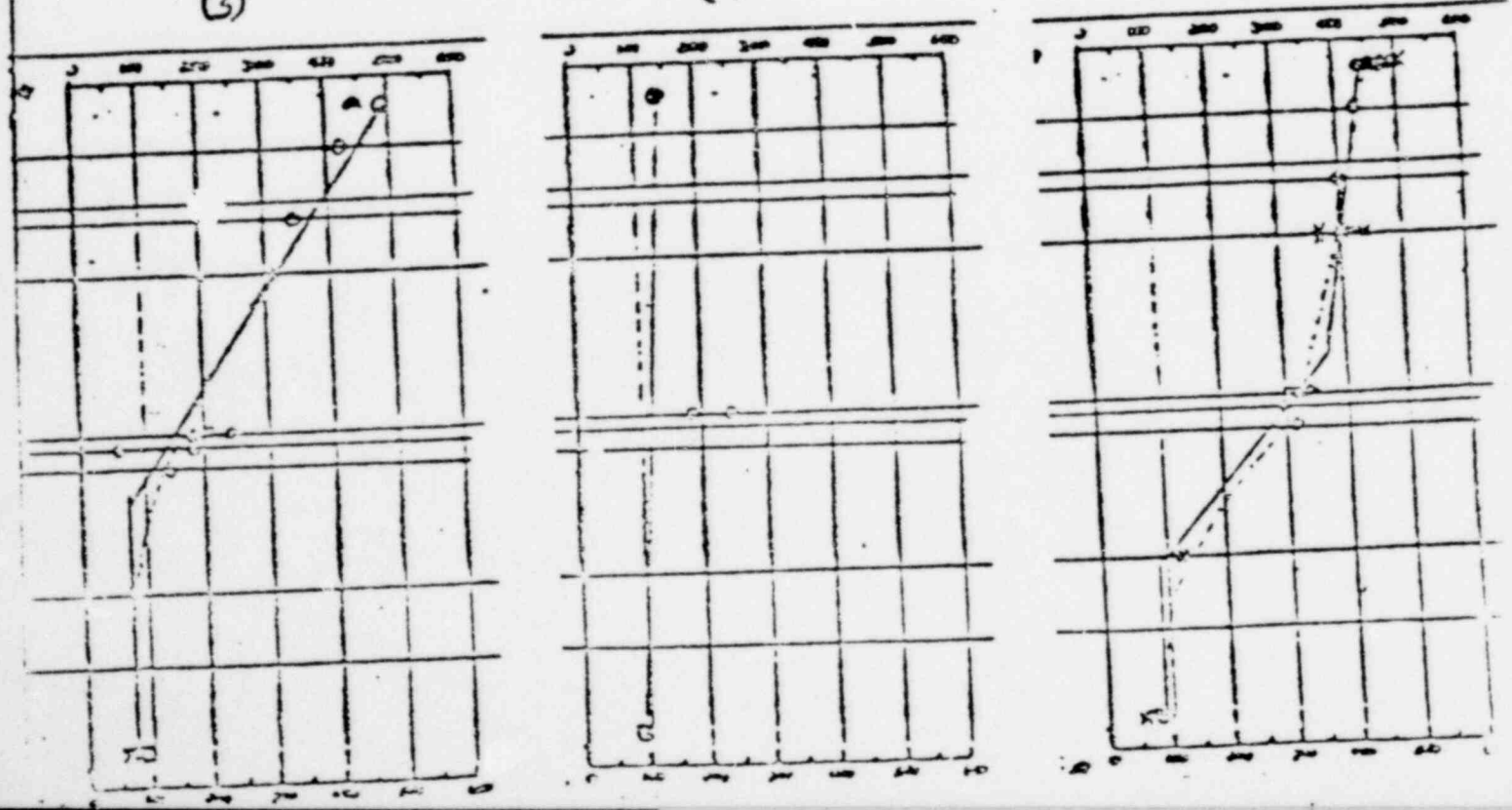

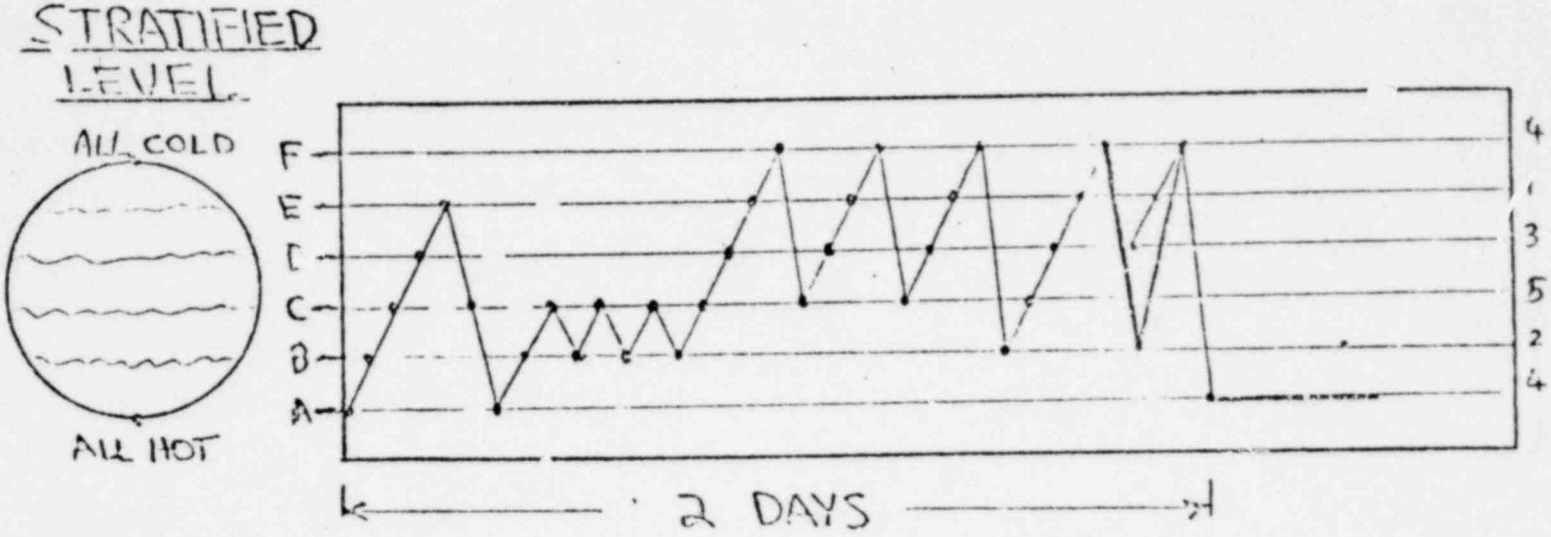

FIGURE 2 · SUMMARY OF TEMPERATURE PROFILE OCCURRENCES

PLANT	EVENT	NUMBER OF OCCURRENCES[1] OF PROFILE					NUMBER[2] OF EVENTS	RANGE[3]	
		1	2	3	4	5		PROFILE 1	PROFILE 2
MILLSTONE (LINE 2) ·	HOT STANDBY	6	6	6	5	9	115	276- 1242	276-1242
			--						

(1) NUMBER OF OCCURRENCES (WITH $\Delta T_{TOP/BOTTOM} \geq 300°F$) IS BASED ON AVAILABLE TEST DATA AND MAY VARY BY $\pm$ 20%.

(2) NUMBER OF EVENTS IS BASED ON PRESENTLY AVAILABLE PLANT OPERATING HISTORY INFORMATION.

(3) RANGE FOR TOTAL NUMBER OF OCCURRENCES OF THE PROFILE AND IS CALCULATED AS: RANGE = (# OF OCCURRENCES $\pm$ 20%) * (# EVENTS) X S, WHERE S = EVENT SIMILARITY FACTOR AND $.5 \leq S \leq 1.5$.

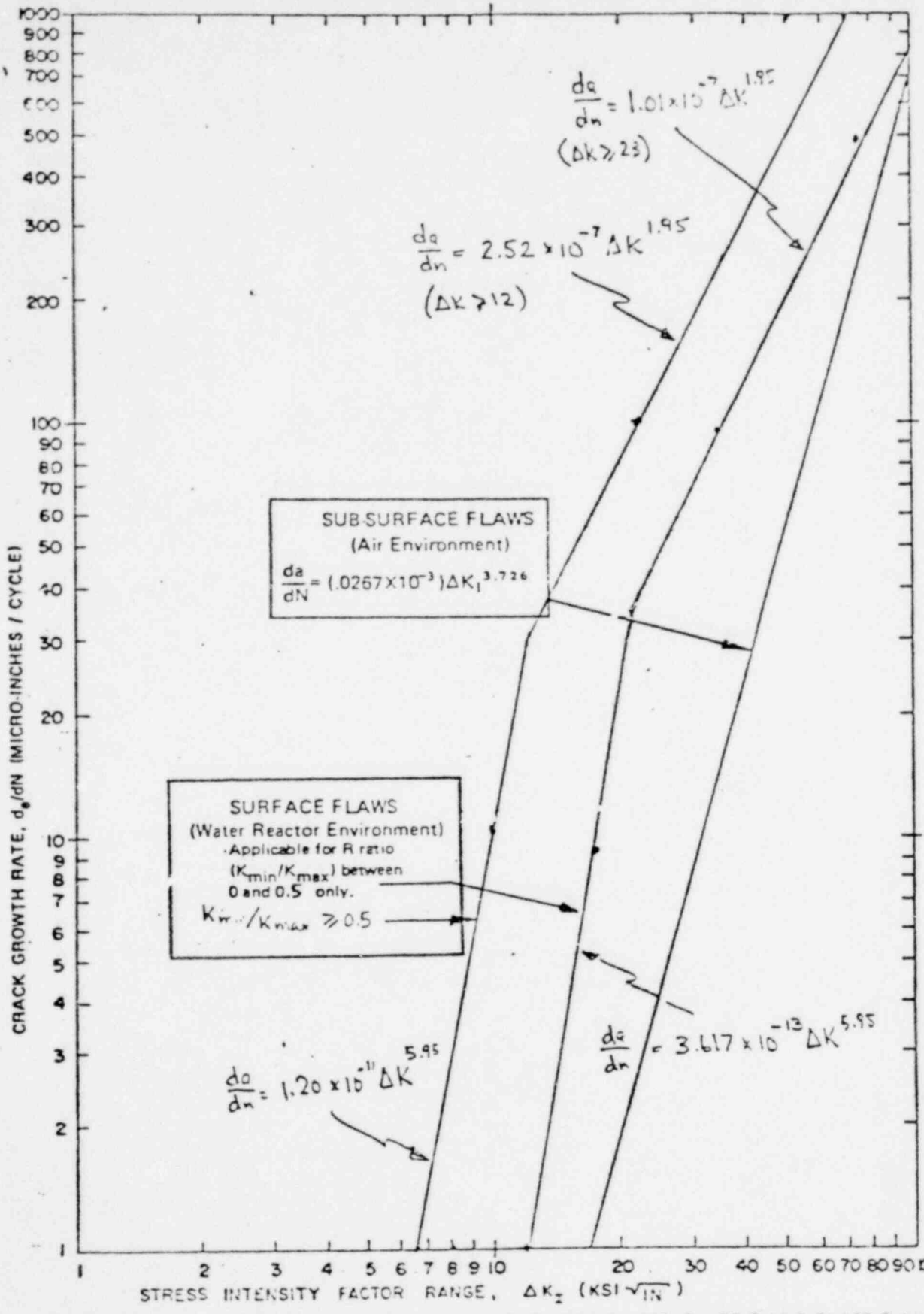

FIGURE 3 FATIGUE CRACK GROWTH DATA FOR SA-508, CLASS 2 AND CLASS 3 AND SA-533, GRADE B, CLASS 1 STEELS

TABLE 2

STRESS RESULTS - AXIAL DIRECTION

CONDITION 5 - 1 - HOT STANDBY # 1

Location	Inside Surface Max. (Ksi)	Inside Surface Min. (Ksi)	Outside Surface Max. (Ksi)	Outside Surface Min. (Ksi)
1	40.0	0.0	-40.0	0.0
2	40.0	0.0	-40.0	0.0
3	9.46	-23.0	8.56	8.29
4	35.12	4.63	11.23	7.02
5	68.97	- 1.43	13.20	4.66
6	66.05	- 7.28	12.61	1.71
7	46.17	- 8.06	10.83	-0.33
8	24.37	7.27	7.34	3.68
9	24.61	7.27	8.98	2.01
10	23.67	- 2.47	6.47	-3.44
11	14.93	- 5.67	- 0.44	-7.05
12	9.30	- 5.44	- 6.03	-8.45
13	7.62	- 7.95	- 8.11	-8.69

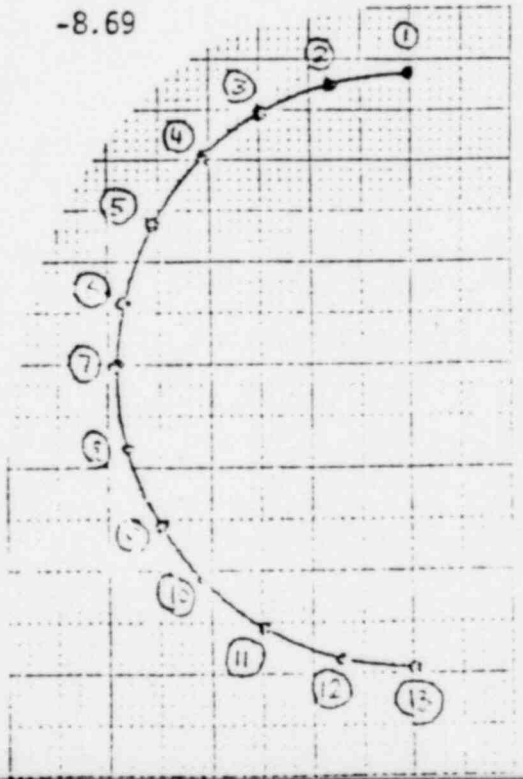

TABLE 1

TRANSIENTS USED IN FATIGUE CRACK GROWTH ANALYSIS

MILLSTONE II

Description	Cycles (40 years)	Inside Surface Stress Max.	Inside Surface Stress Min.	Outside Surface St Max.	
Hot Standby 1	50)				
Hot Standby 2	1500)	These stresses are dependent on circumferent position. See Tables 2 through 5.			
Hot Standby 3	500)				
Hot Standby 4	2500)				
Unit Load-Unload	15000	10.47	7.71	8.49	7
Step Increase/Decrease	2000	9.56	7.87	7.89	7
Partial Loss of Flow	40	23.7	8.42	3.79	7
Loss of Load	40	23.02	8.42	3.18	7
Reactor Trip	400	22.69	8.21	2.88	7
Secondary Leak Test	200	11.23	0.0	10.04	0

TABLE 3

STRESS RESULTS - AXIAL DIRECTION

CONDITION 5 - 4 - HOT STANDBY # 2

Location	Inside Surface Max. (Ksi)	Inside Surface Min. (Ksi)	Outside Surface Max. (Ksi)	Outside Surface Min. (Ksi)
1	13.49	9.78	9.62	3.24
2	12.57	9.68	9.40	3.25
3	9.46	9.34	8.56	3.24
4	8.76	4.63	3.21	7.02
5	8.23	-1.43	3.17	4.60
6	7.91	-7.28	3.17	+1.71
7	7.69	-8.06	3.18	-0.33
8	7.60	7.27	3.22	3.63
9	24.61	7.71	8.97	3.37
10	23.67	8.02	6.47	3.[illegible]3
11	14.93	8.44	-0.44	3.96
12	9.30	8.76	-6.03	4.20
13	7.61	8.86	-8.11	4.29

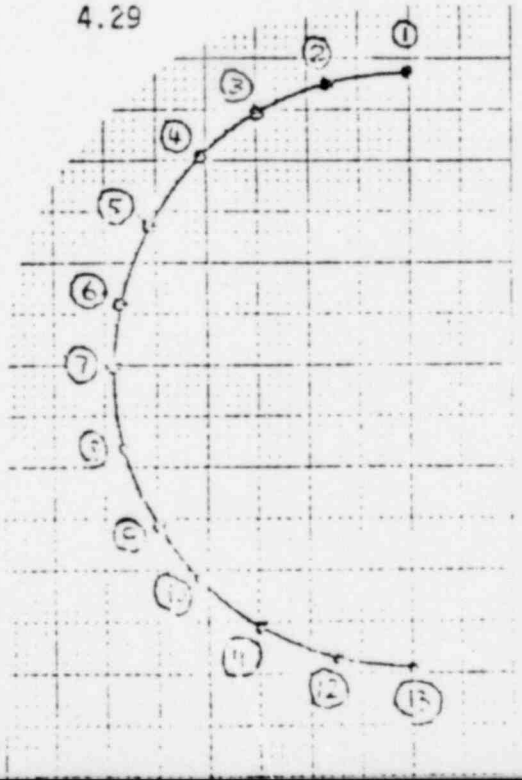

TABLE 4

STRESS RESULTS - AXIAL DIRECTION

CONDITION 2 → 1 - HOT STANDBY # 3

Location	Inside Surface Max. (Ksi)	Inside Surface Min. (Ksi)	Outside Surface Max. (Ksi)	Outside Surface Min. (Ksi)
1	40.0	0.0	-40.0	0.0
2	40.0	0.0	-40.0	0.0
3	16.19	23.71	9.31	8.30
4	35.12	10.11	11.23	8.45
5	68.97	2.39	13.20	6.52
6	66.05	- 4.85	12.61	3.45
7	46.17	-11.04	10.83	-0.88
8	24.37	-15.29	7.34	-5.64
9	7.27	-14.93	2.01	-8.39
10	- 2.48	- 3.19	- 3.44	-4.21
11	19.41	- 5.67	7.35	-7.05
12	36.44	- 5.44	16.75	-8.45
13	41.23	- 4.95	19.41	-8.69

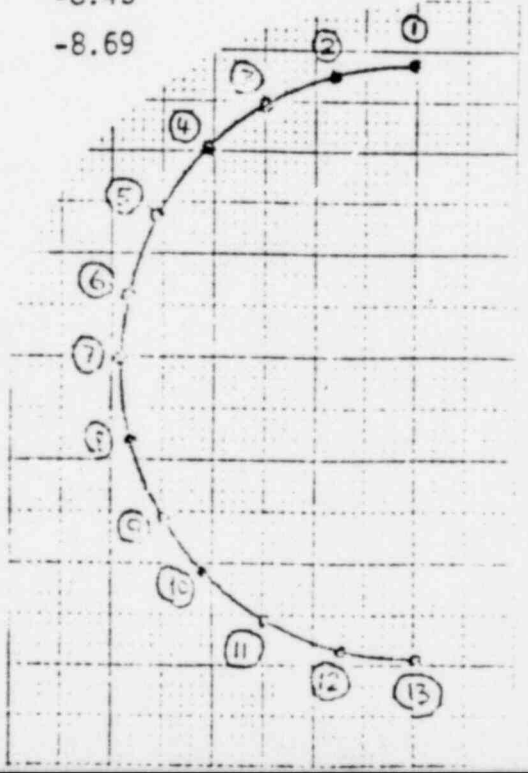

TABLE 5

STRESS RESULTS - AXIAL DIRECTION

CONDITION 2 - 4 - HOT STANDBY # 4

Location	Inside Surface Max. (Ksi)	Inside Surface Min. (Ksi)	Outside Surface Max. (Ksi)	Outside Surface Min. (Ksi)
1	21.51	9.78	9.73	3.24
2	20.0	9.68	9.60	3.24
3	16.19	9.34	9.31	3.24
4	10.11	8.76	8.45	3.21
5	8.23	2.39	3.17	6.52
6	7.91	- 4.88	3.17	3.45
7	7.69	-11.04	3.18	-0.88
8	7.60	-15.29	3.22	-5.64
9	7.71	-14.93	3.37	-8.39
10	8.02	- 3.12	3.63	-4.21
11	19.41	8.44	7.35	3.96
12	36.44	8.76	16.75	4.20
13	41.23	8.85	19.41	4.28

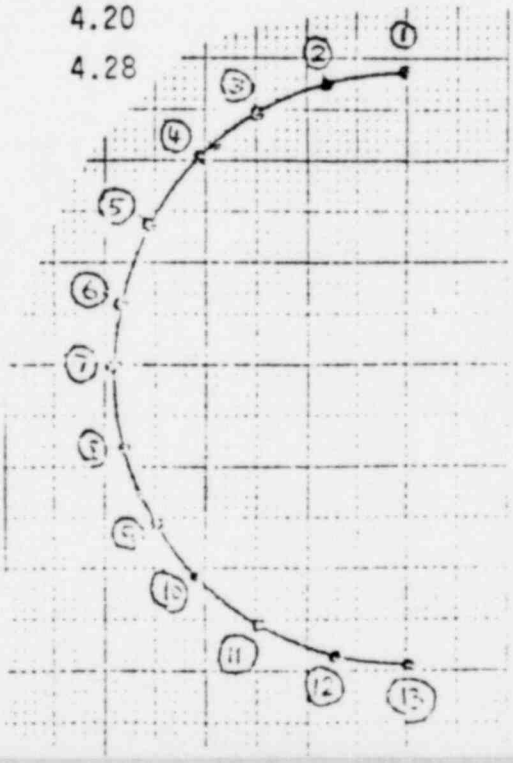

TABLE 6

RESULTS OF FATIGUE CRACK GROWTH ANALYSIS

INITIAL CRACK LENGTH = 0.100 INCHES

Location	Crack Depth After Year			
	.1	2	3	4
1	.1008	.1016	.1024	.1032
2	.1002	.1004	.1007	.1009
3	.1001	.1001	.1002	.1003
4	.1001	.1003	.1004	.1005
5	.1021	.1045	.1067	.1092
6	.1042	.1090	.1137	.1190
7	.1011	.1023	.1034	.1046
8	.1001	.1002	.1003	.1003
9	.1001	.1002	.1003	.1004
10	.1001	.1002	.1002	.1003
11	.1001	.1003	.1004	.1006
12	.1014	.1030	.1045	.1062
13	.1032	.1067	.1105	.1146

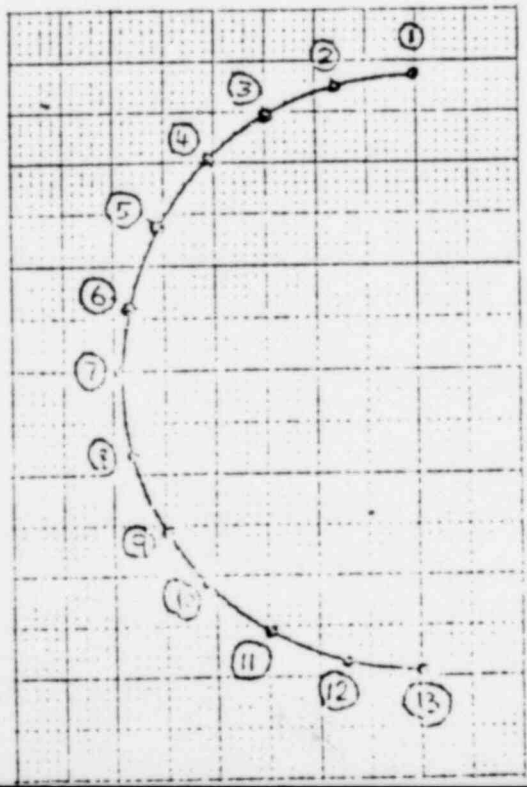

DOCKET NO. 50-336

ATTACHMENT 3

MILLSTONE NUCLEAR POWER STATION, UNIT NO. 2

FEEDWATER SYSTEM PIPING

OCTOBER, 1979

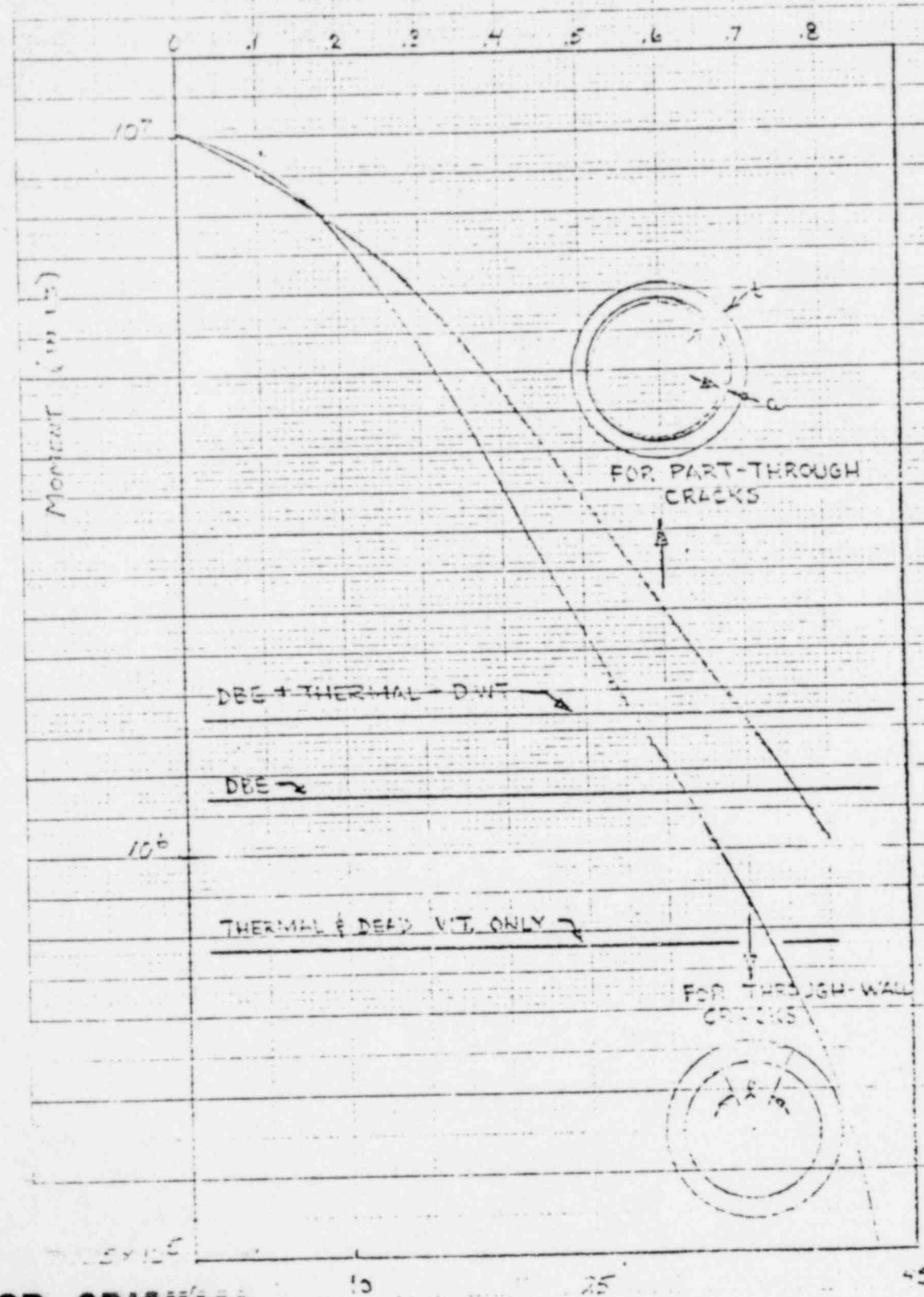

POOR ORIGINAL

1208 274

FIG. 6 FAILURE PREDICTION - 10" OD PIPE 0.75 WALL